ONCOIMMUNOLOGY
2016, VOL. 5, NO. 5, e1112940 (11 pages)
http://dx.doi.org/10.1080/2162402X.2015.1112940

Taylor & Francis
Taylor & Francis Group

ORIGINAL RESEARCH

Anti-α-enolase antibody limits the invasion of myeloid-derived suppressor cells and attenuates their restraining effector T cell response

Paola Cappello[a,b,c], Elisabetta Tonoli[a,b], Roberta Curto[a,b], Daniele Giordano[b], Mirella Giovarelli[a,b,c], and Francesco Novelli[a,b,c,d]

[a]Department of Molecular Biotechnology and Health Sciences, University of Turin, Turin, Italy; [b]Center for Experimental Research and Medical Studies, University Hospital Città della Salute e della Scienza di Torino, Torino, Italy; [c]Molecular Biotechnology Center, via Nizza 52, Torino, Italy; [d]Transplant Immunology Service, University Hospital Città della Salute e della Scienza di Torino, Turin, Italy

ABSTRACT

Pancreatic Ductal Adenocarcinoma (PDA) is a very aggressive tumor for which effective therapeutical strategies are still lacking. Globally, the 5 y survival rate is 5–7% and surgery is the only potentially curative treatment. Immunotherapy represents a novel possibility for treating PDA, and myeloid-derived suppressor cells (MDSC), which are increased in cancer patients and correlate with metastatic burden and cancer stage, offer a new target in cancer therapy. We have previously shown that antibodies against the PDA-associated antigen α-enolase (ENO1) are detected in more than 60% of PDA patients and correlate with a better prognosis. Furthermore, ENO1-DNA vaccination in mice induced anti-ENO1 antibodies that mediated antitumor activity. In this study, the effects of anti-ENO1 binding on MDSC functions and on the T cell response were evaluated. Here, we show that MDSC express ENO1 on their surface, which increased after LPS stimulation. Moreover, anti-ENO1 mAb inhibited adhesion to endothelial cells, as well as *in vitro* and *in vivo* migration. Similarly, after ENO1 mAb treatment of MDSC, arginase activity decreased, while the secretion of pro-inflammatory cytokines (particularly IL-6) increased, and co-stimulatory molecule expression and suppression functions were only partially affected. Finally, we found that activated T cells in the presence of anti-ENO1 mAb-treated MDSC increased IFNγ and IL-17 secretion and decreased IL-10 and TGFβ secretion compared to control MDSC. In conclusion, anti-ENO1 antibodies may inhibit *in vivo* the infiltration into the tumor microenvironment of MDSC, and attenuate their restraining of effector T cell response, opening a new perspective to render PDA immunotherapy more effective.

Abbreviations: ARG-1, arginase-1; BM, bone marrow; ctrlMDSC, unrelated Ab-treated MDSC; ENO1, α-enolase; ENO1-MDSC, anti-ENO1 mAb-treated MDSC; MDSC, myeloid-derived suppressor cells; Tregs, regulatory T cells.

ARTICLE HISTORY
Received 24 July 2015
Revised 20 October 2015
Accepted 22 October 2015

KEYWORDS
α-enolase; cell adhesion; invasion; myeloid-derived suppressor cells; effector T cell response; T cell suppression

Introduction

PDA is very challenging in terms of treatment, with a cure rate of just 7%. Incidence and mortality are almost equivalent, and the incidence has been increasing in recent years. The gold standard cure is surgical resection but this is unfortunately only applied to 20% of patients, although borderline resectable PDA patients underwent to surgery treatment, are increasing.[1] Two effective regimens, namely—gemcitabine/nab-paclitaxel and FOLFIRINOX—have improved outcomes and are being used early in the disease.[2] However, relevant differences in outcomes cannot be implemented without novel strategies. Targeting the immune system is an active area of research, especially after the successful results obtained with immunotherapy in many solid tumors.[3,4]

Immunotherapy includes different approaches that range from passive administration of antibodies, directed, for example, against check-point molecules to impair suppression mechanisms, to active strategies of immunization aimed at improving the host's own immune system stimulation.

Many efforts are still focused on understanding the complex role of the immune system and stromal components in promoting or inhibiting tumor growth. Clinical failure of immunotherapy, which may occur, for example, with cancer vaccines, is often related to the presence of immunosuppressive cells. MDSC are well-characterized regulatory populations, which significantly increase in cancer patients.[5] As MDSC inhibit both the innate and adoptive immunity, they are likely to subvert immune surveillance and prevent an individual's immune system from eliminating newly transformed cells.

Specifically in the case of PDA, MDSC derived from myeloid precursors are recruited in the tumor area by the Kras-mutant-dependent secretion of granulocyte-macrophage colony-stimulating factor (GM-CSF), considering that Kras is mutated in almost 90% of PDA and also present in early human pancreatic intraepithelial neoplasias (PanINs).[6,7] In mice, these immature myeloid cells co-express the markers CD11b and Gr1 and represent a heterogeneous population of cells including precursors to macrophages, dendritic cells and granulocytes at early stages of

CONTACT Paola Cappello paola.cappello@unito.it; Francesco Novelli franco.novelli@unito.it
Supplemental data for this article can be accessed on the publisher's website.

differentiation.[8] In cancer patients, MDSC are typically $CD11b^{+}CD33^{+}CD14^{-}HLA\text{-}DR^{-}$, and can vary their expression of CD15 and other markers.[5] New populations of MDSC have been recently identified in different human tumors,[9] confirming that, similar to mice, different tumors are likely to induce different subtypes of MDSC. Their functional plasticity seems to be due to their ability to acquire different functional profiles in response to different signals, including growth factors, cytokines, hypoxia, environmental acidosis and nutrient deprivation. One of the most characteristic enzymes associated with MDSC suppression functions, namely arginase-1 (ARG1), is modulated by hypoxia inducible factor-1 (HIF-1), which is stabilized in hypoxic conditions. Additional tumor factors affect MDSC maturation, recruitment and margination; however, the exact combination of tumor-derived and environmental factors that regulate MDSC functions, mobilization, proliferation and activation remain poorly understood. In this light, current studies aimed at identifying mechanisms and molecules driving the pro-tumoral skewing and phenotypic heterogeneity of circulating and infiltrating MDSC are of crucial importance in order to develop new immune-based antitumor strategies.

In a previous study, we demonstrated that a DNA vaccination with a plasmid coding for α-enolase (ENO1), a new PDA-associated antigen,[10] significantly prolonged the median survival of engineered mouse models of PDA.[11] This ENO1-DNA vaccine elicited an integrated humoral and cellular antitumor response, and decreased both circulating and infiltrating MDSC and T regulatory cells.[12] In an attempt to enhance the DNA vaccine efficacy, we focused our attention on the effect of antibodies against ENO1 on MDSC mobilization and function. This information will open new perspectives to develop strategies based on the combination of ENO1-DNA vaccine and anti-ENO1 antibodies.

We observed that MDSC expressed surface ENO1, as also demonstrated for monocytes and myeloid cells in a pro-inflammatory environment.[13,14] Due to the role of ENO1 as a plasminogen receptor, crucial for inducing plasmin activation and extracellular matrix degradation, which represent early steps for cellular migration, here we assessed if the anti-ENO1 antibody affected MDSC adhesion, invasion and migration. We also evaluated how cytokine secretion, arginase activity and T cell suppression functions were modulated by anti-ENO1 treatment.

Results

Myeloid-derived suppressor cells increase in PDA patients and tumor-bearing mice and express ENO1 on their surface

Freshly collected blood from PDA patients was stained to analyze the ENO1 expression on $CD11b^{+}CD14^{-}HLA\text{-}DR^{-}CD33^{low}$ cells, which represent human MDSC and are significantly increased in PDA patients compared to age-matched healthy subjects (Table 1 and Fig. 1A). $CD11b^{+}CD14^{-}HLA\text{-}DR^{-}CD33^{hi}$ cells that seem to be not suppressive are actually decreased in PDA patients compared to healthy subjects (Fig. 1A). However, ENO1 is expressed at higher levels on both suppressor and non-suppressor myeloid cells from PDA patients compared to those from healthy subjects (Fig. 1B). Dot plots represent gating strategy to visualized MDSC and histograms report ENO1 expression on $CD33^{low}$ and $CD33^{hi}$ cells respectively (Fig. 1C).

Table 1. Clinical and histological features of PDA patients.

					TNM[a]		
Patient #	Sex	Age at time of diagnosis	Pancreatectomy	Tumor	T	N	M
1	M	60	NO	PDA	CX	C1	C1
2	F	52	NO	PDA	C4	C1	C0
3	F	61	NO	PDA	C4	C1	C1
4	M	76	NO	PDA	CX	CX	C1
5	F	58	NO	PDA	PX	P1	P1
6	F	71	YES	PDA	P3	P0	P0
7	M	59	YES	PDA	P3	P1	P0
8	M	51	YES	PDA	P3	P1	P0
9	M	60	YES	PDA	P2	P1	P0
10	F	73	NO	PDA	PX	P1	P1
11	F	63	YES	PDA	P2	P1	P0
12	M	60	YES	PDA	P2	P1	P0
13	M	47	YES	PDA	P3	P0	P0
14	F	40	NO	PDA	CX	CX	C1
15	F	53	YES	PDA	P3	P0	P0
16	F	73	NO	PDA	C1	CX	C1
17	F	68	NO	PDA	C3	C1	C1
18	F	65	YES	PDA	P3	P1	P0
19	F	79	YES	PDA	P3	P1	P1
21	F	65	NO	PDA	CX	CX	C1
21	M	69	NO	PDA	CX	CX	C1
22	F	65	NO	PDA	C3	C1	C0
23	M	61	YES	PDA	P3	P1	P0
24	F	74	NO	PDA	C3	C1	C1
25	F	69	YES	PDA	P3	P1	P1
26	M	52	NO	PDA	C3	C1	C0

[a] C=clinically defined; P=pathologically defined following surgical resection

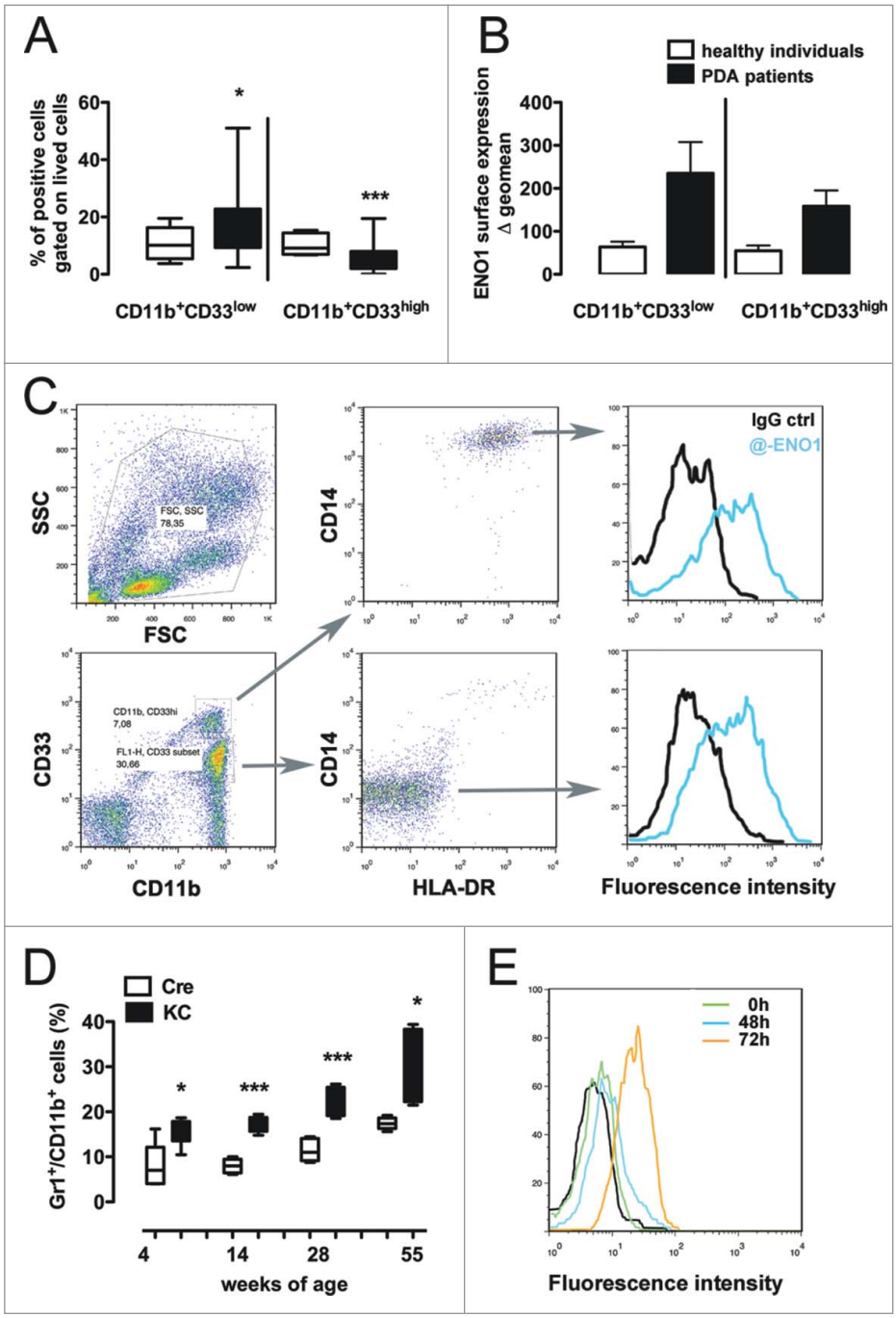

Figure 1. Myeloid-derived suppressor cells express ENO1 on their surface in both PDA patients and tumor-bearing mice. (A) Freshly collected blood from PDA patients and healthy individuals was immediately stained to evaluate the presence of MDSC defined as $CD11b^{+}CD33^{low}CD14^{-}HLA\text{-}DR^{low}$. In the graph, the percentage of $CD11b^{+}CD33^{low}$ or $CD11b^{+}CD33^{high}$ cells is plotted as whiskers from minimun to maximun value for PDA patients (black whiskers) and age-matched healthy individuals (white whiskers). Mean value for each group is also represented. *, $^{***}p$ values < 0.05 and 0.0001 significantly discriminate PDA patients from healthy individuals. (B) ENO1 expression was evaluated on the aforementioned myeloid populations and the geometrical mean intensity of fluorescence was evaluated for each PDA patient (black bars) and age-matched healthy individual (white bars) after subtraction of the fluorescence intensity registered with the isotype IgG (Δ geo mean). Bars represent mean $\pm$ SEM. (C) Dot plots are representative of the gating strategy for the analysis of MDSC in human blood and of ENO1 expression on human MDSC. (C) MDSC defined as $CD11b^{+}Gr1^{+}$ cells were evaluated in the freshly collected blood from KC mice (black whiskers from minimun to maximun value; $n = 5$) and age-matched Cre mice (white whiskers from minimun to maximun value; $n = 5$) at different time point as indicated. *, **, $^{***}p$ values < 0.05, 0.001 and 0.0001 significantly discriminate KC mice from Cre mice. (D) Representative flow cytometry histograms of ENO1 expression on $CD11b^{+}Gr1^{+}$ cells cultured or not (green peak) in the presence of LPS for 48 and 72 h and labeled with an anti-ENO1 mAb (blue and orange line peaks respectively) or an isotype ctrl (black peak). One of three independent flow cytometry evaluations is shown.

Peripheral blood was collected from LSL-$Kras^{G12D}$; Pdx-1/Cre mice (KC) and matched controls Pdx-1/Cre (Cre) at different ages and analyzed for the presence of $CD11b^{+}Gr1^{+}$ cells. KC mice at all time points displayed at least double the percentage of $CD11b^{+}Gr1^{+}$ cells compared to control mice (Fig. 1D). $CD11b^{+}Gr1^{+}$ cells magnetically purified from spleens of KC mice were then analyzed for the presence of ENO1 surface expression after 48 h and 72 h following stimulation with LPS. An increase of ENO1 expression was already observed after 48 h and to a greater extent after 72 h of LPS stimulation (Fig. 1E).

Targeting of surface ENO1 significantly impairs MDSC adhesion to endothelial cells

As the high heterogeneity of *in vivo* MDSC was not easily reproducible during *in vitro* differentiation, we generated MDSC from mouse BM with a well-established protocol from Bronte's group, whereby 85–90% of cells exhibit a continuum of Ly6C and Ly6G expression and retain suppressive activity.[15] Hereafter, we refer to *in vitro*-generated myeloid suppressor cells expanded from the BM as MDSC, although we are aware that this could create a dispute on specific definitions of MDSC accumulating *in vivo* in non-resolving inflammatory sites.

To assess that anti-CD11b or anti-ENO1 antibodies do not affect viability of MDSC, we performed a MTT assay and evaluated the percentage of dying cells by Annexin V staining. MDSC are not proliferating *in vitro* as expected, and no differences in viability were observed between two groups (Fig. S1).

MDSC are recruited from the bloodstream into the tumor area as myeloid precursors that undergo incomplete maturation. To cross the endothelial barrier they roll, and slowly stop in the proximity of tumor area. We therefore first pre-stained MDSC with FITC-conjugated anti-CD11b and then evaluated their ability to adhere to TNF-α-activated syngeneic endothelial cells in the presence (ENO1-MDSC) or absence (ctrlMDSC) of anti-ENO1 mAb. CtrlMDSC adhere well to pre-activated endothelial cells, but adhere significantly less when ENO1 is bound by specific mAb (Fig. 2A, B). Ctrl- and ENO1-MDSC were also assessed for their ability to adhere on different types of extracellular membrane components and no significant differences were observed (Fig. 2C). Of note, both ctrl- and ENO1-MDSC less adhered to all matrix components compared to a tumor cell line, confirming a more invasive and moving phenotype.

Anti-ENO1 mAb strongly decreases the invasive ability of MDSC

To assess the efficacy of anti-ENO1 mAb to inhibit *in vitro* MDSC invasion, matrigel-coated transwells were used for seeding either ctrl- or ENO1-MDSC. After 2 h, non-migrating cells were washed, the matrigel was removed and migrating cells were fixed and stained. Anti-ENO1 mAb dramatically impaired MDSC invasion through the matrigel (Fig. 3A, B). To evaluate the potential *in vivo* significance of our *in vitro* findings, MDSC labeled with the vital dye CytoTrack Red were subcutaneously injected into the hind-leg footpad of mice. After 18 h, the number of MDSC recovered from the draining lymph nodes was evaluated by flow cytometry. We observed a drastic reduction in the number of anti-ENO1-treated MDSC, thus supporting the *in vivo* significance of our *in vitro* results (Fig. 3C). In addition, 8-weeks old C57BL/6 mice were vaccinated with empty or ENO1-expressing plasmid every 2 weeks for a total of three rounds of vaccination and injected with syngeneic PDA cells orthotopically into the pancreas. Thirty days after cell injection, mice were sacrificed and pancreas dissociated to analyze infiltrating immune reactive cells by flow cytometry. As reported in Fig. 3D, ENO1 vaccination induced specific antibodies against the antigen and a significant decrease of myeloid cells into tumor (Fig. 3E).

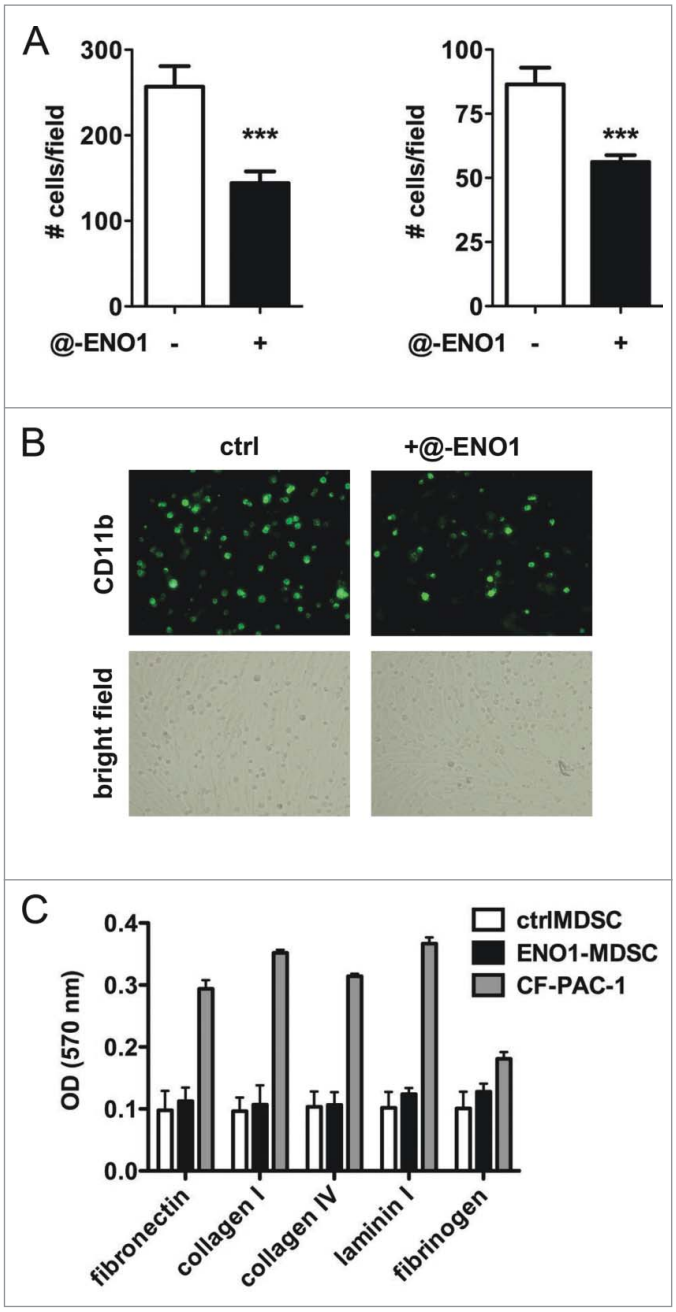

Figure 2. MDSC adhesion to endothelial cells after ENO1-treatment. (A) Bone marrow-generated MDSC were labeled with fluorescein-conjugated anti-CD11b Ab, and untreated or treated with anti-ENO1 mAb before seeding on TNF-α pre-activated endothelial cells for 1 h. Adherent cells were fixed and stained with crystal violet and counted in 10 fields/each condition. Graphs represent the mean ± SEM of two independent experiments in which 6×10^4 and 3×10^4 $CD11b^+$ cells were seeded, respectively. $^{***}p$ values < 0.0001, which significantly discriminate the ctrl- from ENO1-MDSC. (B) Representative pictures of $CD11b^+$ cells untreated or treated with anti-ENO1 mAb in fluorescence (green; upper panels) and of the monolayer of endothelial cells in bright field (lower panels) at 10x magnification. (C) Adhesion to extracellular matrix components was assessed by seeding 1×10^5 cells/well of ctrl- and ENO1-MDSC and CF-PAC-1, as a positive control, in duplicate on a 24-well pre-coated plate. After 90 min, adherent cells were washed and stained. OD was read at 570 nm. Bars represent mean ± SEM.

Effects of ENO1-treatment on cytokine secretion and phenotype marker expression

At 24 h after anti-ENO1 mAb treatment, supernatants from MDSC were collected and evaluated for some of the most common pro- and anti-inflammatory cytokines, such as IL-6, TNF-

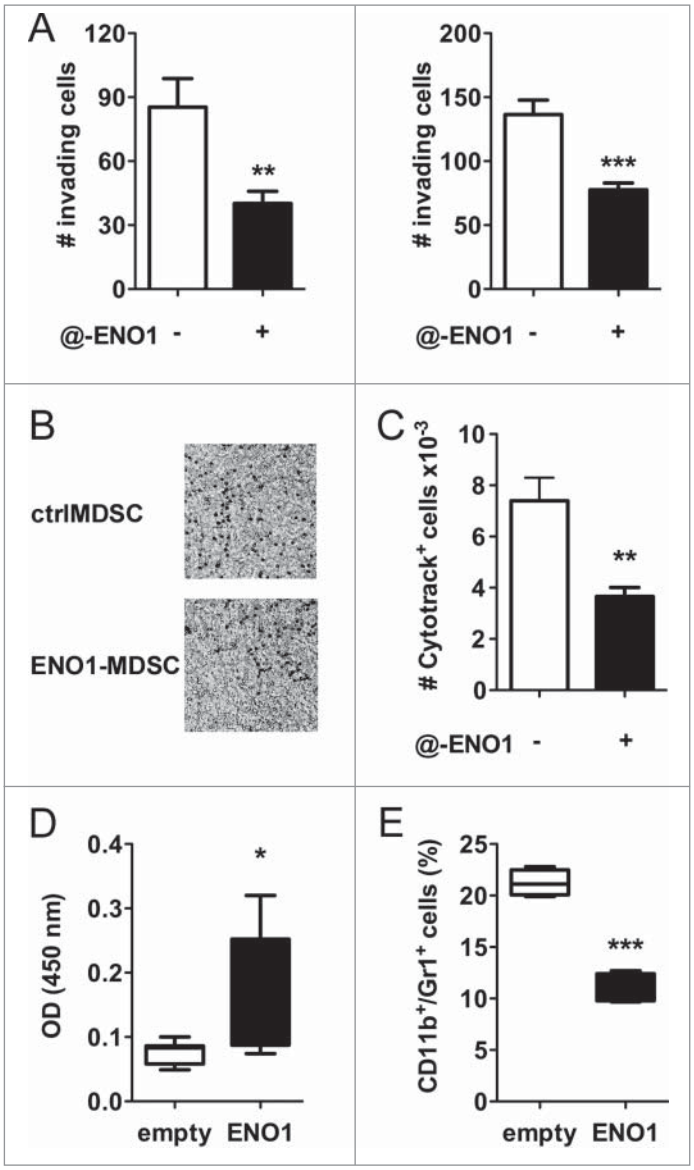

Figure 3. Anti-ENO1 mAb impairs MDSC invasion both *in vitro* and *in vivo*. A. A total of 10^5 and 5×10^4 MDSC were untreated or treated with anti-ENO1 mAb before being seeded on matrigel-coated transwells for 2 h. Invading cells were fixed and stained with crystal violet and counted in 10 fields/each condition. Graphs represent the mean ± SEM of two independent experiments. **, $^{***}p$ values < 0.001 and 0.0001, which significantly discriminate the ctrl- from ENO1-MDSC. (B) Representative pictures of invading ctrl- and ENO1-MDSC after crystal violet staining. Magnification 4x. (C) A total of 2×10^6 of Cytotrack red-labeled ctrl- and ENO1-MDSC were injected subcutaneously into the hind-leg footpad of the mice. The number of MDSC that had migrated to the popliteal lymph nodes was evaluated by flow cytometry. Results are the mean ± SEM of six lymph node samples/group. (D) Sera from vaccinated mice were evaluated for the presence of specific anti-ENO1 antibodies by a direct ELISA. OD values, subtracted of the background values, are plotted as whiskers from minimum to maximum value for ENO1-vaccinated (black whiskers) and empty-vaccinated (white whiskers) mice. Mean value for each group is also represented. $^{*}p$ values < 0.05 significantly discriminate ENO1-vaccinated from empty-vaccinated mice. (E) $CD11b^+Gr1^+$ cells were evaluated in the freshly collected pancreatic tissues. Percentage is plotted as whiskers from minimum to maximum value for empty- (white whiskers) and ENO1-vaccinated (black whiskers) mice. Mean value for each group is also represented. $^{***}p$ values < 0.0001 significantly discriminate ENO1-vaccinated from empty-vaccinated mice.

α, IL-10 and TGF-β. IL-6 was the only cytokine that increased after ENO1-treatment, while TNF-α secretion was reduced, although without statistically significant difference, and no changes were observed for IL-10 or TGF-β (Fig. 4A).

To assess the potential effect of anti-ENO1 mAb on co-stimulatory molecule expression or dendritic cell maturation markers, MDSC were analyzed by flow cytometry at 24 h after ENO1-treatment. Only CD80 was significantly increased after ENO1-treatment (Fig. 4B). In addition, ARG-1 activity was significantly diminished in ENO1-MDSC (Fig. 4C). The increase of IL-6 and not TGF-β suggests a potential impact on Th17 differentiation, while that of CD80, accompanied by the reduction of ARG-1, indicates their ability to sustain T cell effector function.

Analyzing a panel of phospho-proteins revealed an increase of phospho-GSK-3α/β accompanied from a decrease in phospho-p65 NFkB after ENO1-treatment (Fig. 4D). The inhibitory phosphorylation in Ser9 and Ser21 of GSK3α and β respectively can likely be responsible for the decrease in TNF-α secretion, even if not parallel to an increase in IL10.[16] Decrease of TNF-α production eventually correlates with the decrease in phosphorylation of p65 NFkB. However, a GSK3 independent pathway is likely responsible for the induction of IL6 production.

ENO1-treatment does not significantly affect the suppression function but decreases Treg expansion

To assess the effects of ENO1 treatment on MDSC suppressive functions, ctrl- and ENO1-MDSC were co-cultured with lymph node syngeneic T cells activated with anti-CD3 plus anti-CD28 mAbs, and labeled with the vital dye CytoTrack Red. Proliferative cells were detected by flow cytometry after 3 d of culture. As expected, both activated $CD4^+$ and $CD8^+$ T cells were reduced in their ability to proliferate in the presence of MDSC at the ratio 1:1 as shown in Fig. 5A and B. $CD4^+$ and CD^+ activated T cells were able to distribute in four and five generations, respectively, whereas those co-cultured with MDSC were able to divide only two times, irrespective of ENO1-treatment. However, ENO1-MDSC co-cultured T cells secreted significantly more IFNγ and IL-17 and less IL-10 and TGF-β compared to ctrlMDSC co-cultured T cells. Of note, TGF-β decreased to a similar level to that secreted by activated T cells alone (Fig. 5C).

Discussion

It is established that two distinctive hallmarks of tumors are the ability to promote inflammation while avoiding cell disruption.[17] It is also well accepted that tumor-promoting inflammation has detrimental effects on the eliciting of an efficient antitumor response as well as on the efficacy of immunotherapy. However, the existence of a tumor contexture, which is different between tumor types and patients with the same tumor, suggests a specific role for each immune population in tumor onset or progression control.[18] Specifically, myeloid cells (early), and T regulatory cells (later), are the main populations of tumor-infiltrating leukocytes in PDA.[6,8,19]

For many years, we have been focusing efforts in developing novel immunotherapeutical strategies to be applied in the deadliest tumor, namely PDA. We have demonstrated that a DNA vaccine consisting of a necked plasmid coding for ENO1,[11] was

efficient in prolonging mouse survival and eliciting an integrated antitumor response.[11,12,20] One major effect of this response was the limitation of the numbers of MDSC and Tregs both intra-tumoral and in peripheral blood and lymphoid organs.[12] We suggest that the efficacy of the ENO1-vaccine is strongly related to reducing immune suppression, thus facilitating the onset of an effector antitumor response. We have also demonstrated that the anti-ENO1 mAb effectively disturbs the ENO1-plasminogen axis in PDA cells and strongly inhibits their ability to invade and metastasize.[21] ENO1 is also expressed on the cell surface of activated monocytes and macrophages in inflamed tissues, such as synovial fluid in rheumatoid arthritis patients,[14] and we confirmed its expression on BM-generated MDSC as well. Due to the presence of anti-ENO1 auto-antibodies in mice vaccinated with ENO1-DNA, we hypothesized that these antibodies play a role in limiting myeloid suppressor cell infiltration into the tumor area.

Here, we demonstrated that binding of surface ENO1 inhibits MDSC adhesion to pre-activated endothelial cells but not to extracellular matrix components, namely fibronectin, collagen type I and IV and laminin. Anti-ENO1 treatment also decreased the ability of MDSC to invade matrigel and to pass through an endothelial cell monolayer (data not shown). These effects corresponded to a reduced

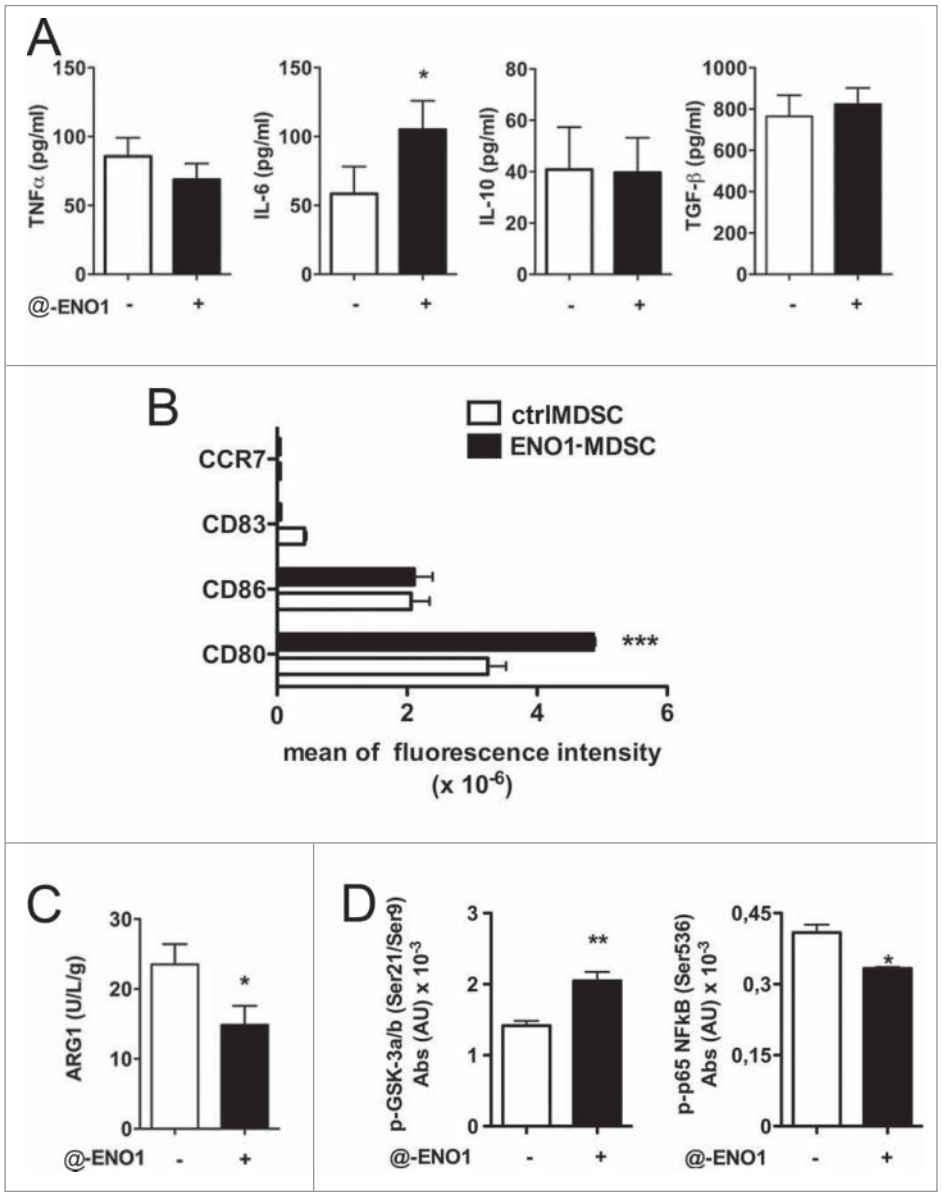

Figure 4. Cytokine secretion and surface marker expression after ENO1-treatment. (A) Bone marrow-generated MDSC were untreated or treated with anti-ENO1 and cultured at 37°C for a further 24 h. Supernatants were collected and evaluated for the presence of TNF-α, IL-6, IL-10 and TGF-β. Graphs represent the mean ± SEM of four independent experiments. $^{*}p$ value < 0.05 which significantly discriminates ctrlMDSC from ENO1-MDSC. (B) Cells were labeled and analyzed by flow cytometry for the expression of indicated co-stimulatory and surface markers. The mean ± SEM of fluorescence intensity from two independent experiments is shown in the graph for ctrl- (white bars) and ENO1-MDSC (black bars). $^{***}p$ value < 0.0001 which significantly discriminates ctrlMDSC from ENO1-MDSC. (C) ARG-1 activity evaluated in ctrl- and ENO1-MDSC lysates. The graph represents the mean ± SEM of values obtained from three independent experiments, $^{*}p$ value < 0.05 which significantly discriminates ctrlMDSC from ENO1-MDSC. (D) Phosphoprotein analysis with total lysate from ctrl- and ENO1-MDSC with the Bio-Plex Pro™ Cell Signaling Assay. Graphs represent the mean ± SEM of fluorescence Absorbance (AU) from phosphoproteins after normalization with total protein concentration. *, $^{**}p$ values < 0.05 and 0.001, which significantly discriminate ctrl- and ENO1-MDSC.

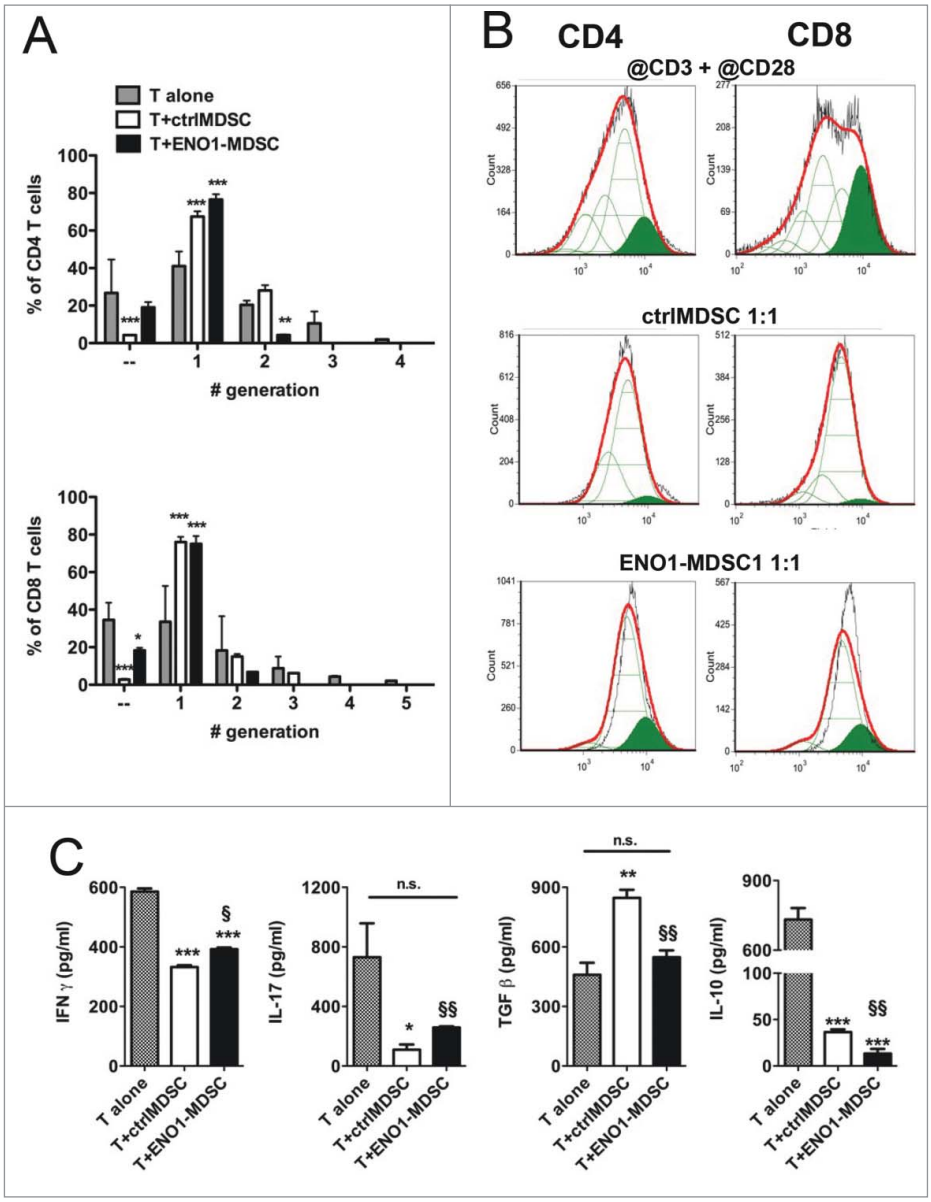

Figure 5. Suppressive function of MDSC after ENO1-treatment. (A) The suppressive function of MDSC was measured using 1×10^6 Cytotrack Red-labeled anti-CD3 plus anti-CD28 mAbs activated lymph node cells, either cultured or not cultured (gray bars) with ctrl- (white bars) or ENO1-MDSC (black bars). Cytotrack Red dilution in both $CD4^+$ and $CD8^+$ T cells was evaluated by flow cytometry. Graphs represent the mean ± SEM of percentage of $CD4^+$ (upper panel) and $CD8^+$ (lower panel) T cells in each generation, as evaluated from the histogram analysis shown in Panel B. *, **, $^{***}p$ values < 0.05, 0.001 and 0.0001 significantly discriminate ctrl- from ENO1-MDSC. (B) Lymph node cells collected after 72 h of co-culture were stained and gated for $CD4^+$ (left panels) and $CD8^+$ (right panels) expression. Green peaks represent the non-dividing population, empty peaks indicate the different generations due to the vital dye dilution and the red line is the fitting curve evaluated by the FCSExpress 5 Software. For the analysis, a ratio of 0.5 between each generation was set. Representative results from two independent experiments are shown. (C) Supernatants from lymph node cells and ctrl- or ENO1-MDSC co-cultures were analyzed for the presence of IFNγ, IL-17, Il-10 and TGF-β. Graphs represent the mean ± SEM of values obtained from three independent experiments. *, **, $^{***}p$ values < 0.05, 0.001 and 0.0001, which significantly discriminate activated T cells alone from those co-cultured with ctrlMDSC and ENO1-MDSC. §, §§p values < 0.05 and 0.001, which significantly discriminate T cells co-cultured with ctrlMDSC from T cells co-cultured with ENO1-MDSC.

ability to invade *in vivo* after injection of MDSC into the footpad of mice. Accordingly, $CD11b^+Gr1^+$ cells were decreased into the tumor of ENO1-vaccinated mice compared to those infiltrating the tumor in empty-vaccinated mice. Taken together, these results suggest that anti-ENO1 auto-antibodies may not only elicit complement or antibody-dependent cytotoxicity of tumor cells[11] and limit tumor metastasis,[21] but also prevent the entrance of myeloid cells into the tumor, where they would tend to be suppressive and contribute to a pro-tumoral environment.

Anti-ENO1 treatment does not, however, inhibit classical suppressive functions of MDSC, namely T cell proliferation; in this case the addition of ENO1-MDSC has a similar effect to that observed in the presence of ctrlMDSC. However, T cells co-cultured with ENO1-MDSC secreted much more Th1/Th17 cytokines and significantly less TGF-β and IL-10. These effects correlated with a lower ARG-1 activity in ENO1-MDSC and a higher expression of the co-stimulatory molecule CD80. ARG-1 has a fundamental role in the urea cycle where it metabolizes L-arginine to L-ornitine and urea, and is also expressed in immune

cells. ARG-1 is believed to play a crucial role in inflammation-induced immune suppression.[22] Depletion of L-arginine by myeloid cells has been accepted as one of the mechanisms by which T cells are suppressed in tumor patients. T cells import L-arginine, and thus, depleting L-arginine significantly inhibits T cell proliferation by inducing cell cycle arrest.[23] In addition, L-arginine deficiency has been shown to downregulate the TCR ζ-chain, which is crucial for TCR signaling.[24] MDSC also impair T cell IFNγ production, and in some studies they have been shown to cause expansion of $CD25^+FoxP3^+$ Tregs.[25] In fact, co-culture of MDSC with naïve T cells stimulated with anti-CD3 and anti-CD28 Abs inhibited the T cell proliferation and impaired IFNγ secretion. Interestingly, ENO1-MDSC although inhibiting T cell proliferation, significantly less affected their IFNγ secretion. Moreover, ENO1-MDSC induced higher levels of IL-17 secretion and decreased the TGF-β secretion compared to ctrlMDSC. These results suggest that anti-ENO1 treatment may skew tumor-specific T cells into effector even when MDSC are recruited in the tumor area.

Several studies have been published demonstrating that stroma depletion[26,27] or myeloid cell impairment[28,29] are efficient in inhibiting PDA growth in preclinical models. The stromal microenvironment is a complex structure composed of an extracellular matrix, activated fibroblasts and myofibroblasts, inflammatory cells and blood and lymphatic vessels, which differently shape the normal architecture of pancreatic tissue.[30] Although this extensive stroma has been considered the major cause for chemoresistance,[31] the downside was that desmoplastic reactions and stroma would prevent formation of metastases. Unfortunately, this idea has been abandoned in place of a more recent hypothesis that stroma promotes tumor growth and invasion. However, a recent paper has demonstrated that the Sonic Hedgehog (Shh) pathway is crucial for inducing a desmoplastic response, but also highlights that stromal elements are important to restrain neo-angiogenesis and, as a consequence, tumor growth.[32] Similar reports came from another study in which authors demonstrated that depleting myofibroblasts correlated with reduced survival, tumor undifferentiating, invasion and increased epithelial-to-mesenchymal transition.[33] Therefore, both studies underscore the need for caution in targeting carcinoma-associated fibroblasts. Depletion of myeloid cells, by pharmacological approaches, was instead efficient in increasing intratumoral accumulation of activated $CD8^+$ T cells, apoptosis of tumoral cells and shaping of tumor stroma.[29] In addition, a previous study has demonstrated that inhibiting myeloid cell adhesion and invasion by treating with a PI3Kγ inhibitor was sufficient to impair tumor growth.[28]

Accordingly, anti-ENO1 antibodies appear to be useful to limit invasion and migration of both myeloid suppressor cells and tumor cells, thus potentially avoiding or restraining immune suppression and inhibiting tumor metastasis, which, in turn, would be favored by the desmoplastic response. These results also explain why PDA patients with autoantibodies against ENO1 tend to display a better prognosis.[34] Therefore, we suggest that anti-ENO1 mAbs could represent a novel therapeutical strategy. ENO1-treated MDSC invaded to a lesser extent, but secreted pro-inflammatory cytokines and displayed a decreased ARG-1 activity. These features favor the Th1/Th17 T cell skewing, and their specific cytokines may help the switching of auto-antibodies toward those more effective in mediating tumor lysis. Moreover, T cells co-cultured with ENO1-MDSC secreted significantly less TGF-β, which may promote Th17 differentiation *in vivo* due the presence of IL6. In addition, TGF-β does not suppress infiltrating tumor T cells directly or by stabbing DC, and does not elicit T naïve conversion into induced Tregs, further increasing immunosuppression.[35] Treatment with anti-ENO1 antibodies may represent a new immunotherapeutic option to prolong survival in metastatic PDA patients, in combination with canonical chemotherapeutical treatments, or to avoid recurrence and tumor spreading in resectable PDA patients. Anti-ENO1 antibodies may also be actively elicited by vaccination against ENO1.

Materials and methods

Evaluation of human and mouse MDSC

Human and mouse MDSC were analyzed by staining whole blood after red cell lysis with 0.83% NH_4Cl^-0.1% KHCO3-0.04% EDTA buffer and washing with PBS-0.5% BSA-0.02% NaN_3. The following mAbs were used after blocking non-specific sites with rabbit IgG (Dako; X090302-8) and anti-CD16/CD32 (Miltenyi; 130-092-574) mAb, respectively: CD14 (Miltenyi; 130-098-070), CD15 (Dako; F0830), CD33 (BD; 345799) and CD124 (R&D Systems; FAB230P) for human MDSC and CD11b (Miltenyi; 130-081-201) and Gr1 (Biolegend; 108408) for mouse MDSC. After washing, cells were acquired and analyzed with a FACSCalibur and FlowJo Software (both from BD). A total of 50,000 CD11b-gated cells were acquired for each sample.

Blood for healthy controls was collected from volunteers with an age ranging from 53 to 60 y (4F; 6M), while PDA patient blood was collected after signing a consensus based on the protocol accepted by our Hospital Ethics Committee (age range: 42–81 y old; 16F and 10M).

MDSC generation

MDSC were generated from bone marrow cells isolated from tibiae and femurs from C57BL/6 mice maintained in the Animal Facility at the Molecular Biotechnology Center, Turin, in accordance with the European guidelines and protocols approved by the Institutional Animal Care. Red blood cells were lysed with ammonium chloride. To obtain bone marrow-derived MDSC, 2.5×10^6 cells were plated into 10 mm-diameter dishes in 10 mL of RPMI-10% FBS-2.6×10^{-5} M β-mercaptoethanol supplemented with GM-CSF (40 ng/mL; Miltenyi, 130-095-746) and IL-6 (40 ng/mL; Peprotech by Tebu-Bio, 216–16). Cells were maintained at 37°C in a 5% CO_2-humidified atmosphere for 4 d Collected cells were labeled with FITC-conjugated anti-CD11b antibody (Miltenyi) and divided into two groups with or without the addition of anti-ENO1 mAb (clone V15, SantaCruz). The first group incubated with anti-CD11b only was called "ctrlMDSC" and the second group was called "ENO1-MDSC." The presence of anti-CD11b in ctrMDSC rule out confounding effects due to the FcγR interaction.

In vitro adhesion assay

Murine endothelial cells (1×10^5/well; MS-1 CRL-2279™ from ATCC) were seeded in a 24-well plate, stimulated with murine recombinant TNFα (50ng/mL; Peprotech by Tebu-Bio, 315–01A), and incubated at 37°C. After 24 h, cells were washed with sterile DPBS (Sigma, D8537) and anti-CD16/CD32 (Miltenyi; 130-092-574) mAb was added for 30 min on ice. Ctrl- and ENO1-treated MDSC were seeded on top of the endothelial cells in triplicate at two different concentrations (3×10^4 and 6×10^4/well) and then incubated for 90 min at 37°C. Non-adherent cells were removed by washing with DPBS and adherent cells were fixed with 2% formaldehyde (Bio-Optica; 05-01005q). Cells were observed under a fluorescent microscope equipped with a camera (Leica); 10 fields/well were recorded as jpg images and adherent cells were counted with the ImageJ Software.

Ctrl- and ENO1-MDSC were evaluated for their ability to adhere to different extracellular matrix components using the CytosSelect™ 48-well Cell Adhesion Assay (ECM Array, Colorimetric Format) (Cell Biolabs, Inc., CBA-070) following the manufacturer's instructions. PDA tumor cells, namely CF-PAC-1 (ECACC Ref. No: 91112501), were used as a positive control. A total of 100,000 cells were seeded in each well and left to adhere for 90 min at 37°C. Extracted samples were transferred to a 96-well plate and OD was read at 570 nm in a plate reader (BioRad).

In vitro invasion assay

Transwells (8 μm pore size; Corning Inc, 3422) were placed in a 24-well plate, coated with 50μL of Matrigel (BD, 356234), diluted at 1:8 in serum-free RPMI, and incubated for 4 h at 37°C to allow solidification. Transwells were then transferred into a new 24-well plate containing 0.6 mL/well of RPMI supplemented with 30% FBS. Ctrl- and ENO1-MDSC were seeded at two different concentrations in duplicate in serum-free medium in the upper chambers (5×10^4 and 1×10^5/well). Plates were incubated for 2 h at 37°C. The non-invading cells were scraped from the top of the transwells with a cotton swab. Invasive cells were fixed for 30 min with 2% glutaraldehyde (Sigma, 3G-6403) and stained for 30 min with Crystal Violet (Sigma; V5265). The invasive cells were observed under a light microscope equipped with a camera (Leica); 10 fields/well were recorded as jpg images and invading cells were quantified with the ImageJ Software.

In vivo MDSC migration

MDSC were labeled with the vital dye Cytotrack Red (Bio-Rad, 135-1202-135-1205) following the manufacturer's instructions. A total of 2×10^6 labeled cells were injected subcutaneously into the two hind leg footpads in 3 mice/group. Popliteal lymph nodes were collected 18 h later, mechanically disaggregated, and cell suspensions were further stained with FITC-conjugated anti-CD11b (Miltenyi, 130-081-201) for the examination and quantitation by flow cytometry (FACScanto, BD).

ENO1-DNA vaccination in mice

Eight-weeks old C57BL/6 mice were vaccinated with empty or ENO1-expressing pVAX vector as previously described.[11] Mice were vaccinated every two weeks for a total of three rounds of vaccination. Two weeks after the last vaccination mice were injected orthotopically into the pancreas with 1×10^5 syngeneic PDA cells. Thirty days after cell injection, mice were sacrificed, tumor excised and immediately processed to obtain a single cell suspension for flow cytometry analysis. Briefly, 0.5-1 g of PDA was dissociated in sterile 10 cm dish with ~1 mL cold dissociation buffer (DPBS containing 0.5 mg/mL of collagenase IV, 0.1 mg/mL of Hyaluronidase V, 0.6 U/mL of Dispase II, 0.005 MU/mL of DNAse I and 0.2 mg/mL of Soybean Tryspin inhibitor) by using a steril razor blade. Resuspended tissue was transferred into a clean tube and placed at 37°C for 15 min, by pipetting twice during the incubation. Cell suspension was filtered with a 70 mm filter into DPBS-0.5% BSA-2mM EDTA buffer and washed with with DPBS-0.5% BSA-0.02% sodium azide. After incubation with purified anti-CD16/32 (Miltenyi, 130-092-574) on ice for 5 min to block non-specific binding, cells were incubated with fluorocrome-conjugated anti-CD11b, anti-Gr1 (Biolegend, 108 408), anti-CD115 (Miltenyi, 130-102-504), anti-Ly6G (Miltenyi, 130-093-140), anti-Ly6C (Miltenyi, 130 102-295) and anti-F4/80 (eBioscience, 15-4801-82) for a further 30 min. After washing, cells were acquired with an AccuriC6 (BD) and analyzed by FlowJo (by BD, Milan, Italy).

Two weeks after the last vaccination, sera were collected and assessed for the presence of anti-ENO1 specific IgG by a direct ELISA as previously reported.[11]

Analyses of cytokines, surface markers and phosphoproteins

Ctrl- and ENO1-MDSC were maintained in sterile polypropylene round-bottom tubes in complete medium for 18h at 37°C in a 5% CO_2-humidified atmosphere. Supernatants were collected and analyzed for the presence of TNF-α (R&D System, DY410), IL-6 (Biolegend, 431302), IL-10 (R&D System, DY417) and TGF-β (R&D System, DY679) by ELISA following the manufacturer's instructions. For surface marker analyses, cells were harvested, washed with DPBS-0.5% BSA-0.02% sodium azide, incubated with purified anti-CD16/32 (Miltenyi, 130-092-574) on ice for 5 min to block non-specific binding and with anti-CD80 (BD, 553768), CD83 (Biolegend, 121509), CD86 (Biolegend, 105011), and CCR7 (eBiosciences, 17–1971–81) for a further 30 min. After washing, cells were acquired with an AccuriC6 (BD) and analyzed by FlowJo (by BD, Milan, Italy).

To analyze phosphoproteins, ctrl- and ENO-MDSC were washed, and pellets were frozen until use. Bioclarma Lab (Turin, Italy) analyzed lysates in duplicate with the Bio-Plex ProTM Cell Signaling Assay (Bio-Rad, 171-V50000), customized for the detection of phospho-GSK-3a/b (Ser21/Ser9) and p65 NFkB (Ser536) and provided data on fluorescence intensities and protein concentrations.

To analyze arginase activity, cells were washed with DPBS and pellets were frozen until use. After thawing and lysing pellets with the lysis buffer contained in the QuantiChrom

Arginase Assay Kit (BioAssay Systems, DARG200), protein concentration was evaluated with the CB-X assay (G-Biosciences by VWR, Milan, Italy) to normalize ARG-1 activity to total protein concentration. The following formula was applied to evaluate the activity of ARG-1:

$$\begin{aligned}\text{Arginase} &= (\text{OD sample} - \text{OD blank}) \\ &\quad /(\text{OD standard} - \text{OD water}) \\ &\quad \times[\text{Urea standard}]\times 50\times 10^3/(40\times t) \\ &= (\text{OD sample} - \text{OD blank}) \\ &\quad /(\text{OD standard} - \text{OD water})\times 10.4\ (\text{U/L}),\end{aligned}$$

where OD sample, OD blank, OD standard and OD water were the optical density values of the sample, blank, standard and water, respectively, read at 430 nm with a microplate reader (BioRad). [Urea standard] = 1mM, t is the reaction time (120 min). 50 and 40 are the reaction and sample volumes (μL), respectively.

Polyclonal T Cell suppression assays

Lymph node cells from C57BL/6 mice were labeled with CytoTrack Red dye, washed and added (1×10^6 cells/well) to all wells in a 24-well plate. Cells were stimulated with plate-bound anti-CD3 (0.5 μg/mL; 100302) and soluble anti-CD28 (3 μg/mL; 102102), both purchased from Biolegend. Ctrl- and ENO1-MDSC were added at ratios of 1:1 and 1:4, respectively, to lymph node cells, in triplicate. Proliferation of $CD4^+$ and $CD8^+$ T cells was evaluated by flow cytometry after 72 h. Cells were harvested and labeled with FITC-conjugated anti-CD4 (Miltenyi, 130-091-608) and PerCP-conjugated anti-CD8 (Miltenyi, 130-094-960) in order to gate dye dilution histograms on $CD4^+$ and $CD8^+$ cells, respectively. Cells were acquired with an AccuriC6 instrument and analyzed with the FCS Express 4 Software.

Supernatants from co-cultures were collected at 72 h and analyzed for the presence of IFNγ (DY485), IL-17 (DY421), IL-10 (DY417) and TGF-β (DY679), by ELISA, following the manufacturer's instructions (all purchased from R&D System).

Statistical analysis

All the experiments were repeated at least three times with MDSC generated from pooled BM cells, if not indicated differently. Two-tailed Student's *t* test or Mann–Whitney–Wilcoxon test were used for evaluating statistical significance between groups, as indicated.

Disclosure of potential conflicts of interest

No potential conflicts of interest were disclosed.

Acknowledgments

We thank Dr. Radhika Srinivasan for critical reading of the manuscript.

Funding

This study was supported by Associazione Italiana Ricerca sul Cancro (5 × mille no. 12182) and (IG no. 15257); University of Turin-Progetti Ateneo 2014-Compagnia di San Paolo (PANTHER for P.C.) (PC-METAIMMUNOTHER for F.N.); Fondazione Ricerca Molinette.

References

1. Malafa MP. Defining borderline resectable pancreatic cancer: emerging consensus for an old challenge. J Natl Compr Cancer Netw 2015; 13:501-4; PMID:25964634
2. Vaccaro V, Sperduti I, Vari S, Bria E, Melisi D, Garufi C, Nuzzo C, Scarpa A, Tortora G, Cognetti F et al. Metastatic pancreatic cancer: Is there a light at the end of the tunnel? World J Gastroenterol 2015; 21:4788-801; PMID:25944992; http://dx.doi.org/10.3748/wjg.v21.i16.4788
3. Gravitz L. Cancer immunotherapy. Nature 2013; 504:S1; PMID:24352357; http://dx.doi.org/10.1038/504S1a
4. Tempero MA. Multidisciplinary management of pancreatic cancer. J Natl Compr Cancer Netw 2015; 13:700-2; PMID:25995435
5. Ostrand-Rosenberg S, Sinha P. Myeloid-derived suppressor cells: linking inflammation and cancer. J Immunol 2009; 182:4499-506; PMID:19342621; http://dx.doi.org/10.4049/jimmunol.0802740
6. Bayne LJ, Beatty GL, Jhala N, Clark CE, Rhim AD, Stanger BZ, Vonderheide RH. Tumor-derived granulocyte-macrophage colony-stimulating factor regulates myeloid inflammation and T cell immunity in pancreatic cancer. Cancer Cell 2012; 21:822-35; PMID:22698406; http://dx.doi.org/10.1016/j.ccr.2012.04.025
7. Clark CE, Beatty GL, Vonderheide RH. Immunosurveillance of pancreatic adenocarcinoma: insights from genetically engineered mouse models of cancer. Cancer Lett 2009; 279:1-7; PMID:19013709; http://dx.doi.org/10.1016/j.canlet.2008.09.037
8. Pylayeva-Gupta Y, Lee KE, Hajdu CH, Miller G, Bar-Sagi D. Oncogenic Kras-induced GM-CSF production promotes the development of pancreatic neoplasia. Cancer Cell 2012; 21:836-47; PMID:22698407; http://dx.doi.org/10.1016/j.ccr.2012.04.024
9. Talmadge JE, Gabrilovich DI. History of myeloid-derived suppressor cells. Nat Rev Cancer 2013; 13:739-52; PMID:24060865; http://dx.doi.org/10.1038/nrc3581
10. Cappello P, Tomaino B, Chiarle R, Ceruti P, Novarino A, Castagnoli C, Migliorini P, Perconti G, Giallongo A, Milella M et al. An integrated humoral and cellular response is elicited in pancreatic cancer by α-enolase, a novel pancreatic ductal adenocarcinoma-associated antigen. Int J Cancer 2009; 125:639-48; PMID:19425054; http://dx.doi.org/10.1002/ijc.24355
11. Cappello P, Rolla S, Chiarle R, Principe M, Cavallo F, Perconti G, Feo S, Giovarelli M, Novelli F. Vaccination With ENO1 DNA Prolongs Survival of Genetically Engineered Mice With Pancreatic Cancer. Gastroenterology 2013; 144(5):1098-106; PMID:23333712; http://dx.doi.org/10.1053/j.gastro.2013.01.020.
12. Cappello P, Novelli F. A self antigen reopens the games in pancreatic cancer. Oncoimmunology 2013; 2:e24384; PMID:23894698; http://dx.doi.org/10.4161/onci.24384
13. Wygrecka M, Marsh LM, Morty RE, Henneke I, Guenther A, Lohmeyer J, Markart P, Preissner KT. Enolase-1 promotes plasminogen-mediated recruitment of monocytes to the acutely inflamed lung. Blood 2009; 113:5588-98; PMID:19182206; http://dx.doi.org/10.1182/blood-2008-08-170837
14. Bae S, Kim H, Lee N, Won C, Kim HR, Hwang YI, Song YW, Kang JS, Lee WJ. α-Enolase expressed on the surfaces of monocytes and macrophages induces robust synovial inflammation in rheumatoid arthritis. J Immunol 2012; 189:365-72; PMID:22623332; http://dx.doi.org/10.4049/jimmunol.1102073
15. Marigo I, Bosio E, Solito S, Mesa C, Fernandez A, Dolcetti L, Ugel S, Sonda N, Bicciato S, Falisi E et al. Tumor-induced tolerance and immune suppression depend on the C/EBPbeta transcription factor. Immunity 2010; 32:790-802; PMID:20605485; http://dx.doi.org/10.1016/j.immuni.2010.05.010

16. Wang H, Brown J, Martin M. Glycogen synthase kinase 3: a point of convergence for the host inflammatory response. Cytokine 2011; 53:130-40; PMID:21095632; http://dx.doi.org/10.1016/j.cyto.2010.10.009
17. Hanahan D, Weinberg RA. Hallmarks of cancer: the next generation. Cell 2011; 144:646-74; PMID:21376230; http://dx.doi.org/10.1016/j.cell.2011.02.013
18. Fridman WH, Pages F, Sautes-Fridman C, Galon J. The immune contexture in human tumours: impact on clinical outcome. Nat Rev Cancer 2012; 12:298-306; PMID:22419253; http://dx.doi.org/10.1038/nrc3245
19. Clark CE, Hingorani SR, Mick R, Combs C, Tuveson DA, Vonderheide RH. Dynamics of the immune reaction to pancreatic cancer from inception to invasion. Cancer Res 2007; 67:9518-27; PMID:17909062; http://dx.doi.org/10.1158/0008-5472.CAN-07-0175
20. Chu NJ, Armstrong TD, Jaffee EM. Nonviral oncogenic antigens and the inflammatory signals driving early cancer development as targets for cancer immunoprevention. Clin Cancer Res 2015; 21:1549-57; PMID:25623216; http://dx.doi.org/10.1158/1078-0432.CCR-14-1186
21. Principe M, Ceruti P, Shih NY, Chattaragada MS, Rolla S, Conti L, Bestagno M, Zentilin L, Yang SH, Migliorini P et al. Targeting of surface α-enolase inhibits the invasiveness of pancreatic cancer cells. Oncotarget 2015; 6:11098-113; PMID:25860938; http://dx.doi.org/10.18632/oncotarget.3572
22. Munder M. Arginase: an emerging key player in the mammalian immune system. Br J Pharmacol 2009; 158:638-51; PMID:19764983; http://dx.doi.org/10.1111/j.1476-5381.2009.00291.x
23. Rodriguez PC, Quiceno DG, Ochoa AC. L-arginine availability regulates T-lymphocyte cell-cycle progression. Blood 2007; 109:1568-73; PMID:17023580; http://dx.doi.org/10.1182/blood-2006-06-031856
24. Rodriguez PC, Zea AH, DeSalvo J, Culotta KS, Zabaleta J, Quiceno DG, Ochoa JB, Ochoa AC. L-arginine consumption by macrophages modulates the expression of CD3 zeta chain in T lymphocytes. J Immunol 2003; 171:1232-9; PMID:12874210; http://dx.doi.org/10.4049/jimmunol.171.3.1232
25. Hoechst B, Ormandy LA, Ballmaier M, Lehner F, Kruger C, Manns MP, Greten TF, Korangy F. A new population of myeloid-derived suppressor cells in hepatocellular carcinoma patients induces CD4(+)CD25(+)Foxp3(+) T cells. Gastroenterology 2008; 135:234-43; PMID:18485901; http://dx.doi.org/10.1053/j.gastro.2008.03.020
26. Beatty GL, Chiorean EG, Fishman MP, Saboury B, Teitelbaum UR, Sun W, Huhn RD, Song W, Li D, Sharp LL et al. CD40 agonists alter tumor stroma and show efficacy against pancreatic carcinoma in mice and humans. Science; 331:1612-6; PMID:21436454; http://dx.doi.org/10.1126/science.1198443
27. Feig C, Jones JO, Kraman M, Wells RJ, Deonarine A, Chan DS, Connell CM, Roberts EW, Zhao Q, Caballero OL et al. Targeting CXCL12 from FAP-expressing carcinoma-associated fibroblasts synergizes with anti-PD-L1 immunotherapy in pancreatic cancer. Proc Natl Acad Sci U S A 2013; 110:20212-7; PMID:24277834; http://dx.doi.org/10.1073/pnas.1320318110
28. Schmid MC, Avraamides CJ, Dippold HC, Franco I, Foubert P, Ellies LG, Acevedo LM, Manglicmot JR, Song X, Wrasidlo W et al. Receptor tyrosine kinases and TLR/IL1Rs unexpectedly activate myeloid cell PI3kgamma, a single convergent point promoting tumor inflammation and progression. Cancer Cell 2011; 19:715-27; PMID:21665146; http://dx.doi.org/10.1016/j.ccr.2011.04.016
29. Stromnes IM, Brockenbrough JS, Izeradjene K, Carlson MA, Cuevas C, Simmons RM, Greenberg PD, Hingorani SR. Targeted depletion of an MDSC subset unmasks pancreatic ductal adenocarcinoma to adaptive immunity. Gut 2014; 63:1769-81; PMID:24555999; http://dx.doi.org/10.1136/gutjnl-2013-306271
30. Neesse A, Michl P, Frese KK, Feig C, Cook N, Jacobetz MA, Lolkema MP, Buchholz M, Olive KP, Gress TM. Stromal biology and therapy in pancreatic cancer. Gut 2011; 60:861-8; PMID:20966025; http://dx.doi.org/10.1136/gut.2010.226092
31. Olive KP, Jacobetz MA, Davidson CJ, Gopinathan A, McIntyre D, Honess D, Madhu B, Goldgraben MA, Caldwell ME, Allard D et al. Inhibition of Hedgehog signaling enhances delivery of chemotherapy in a mouse model of pancreatic cancer. Science 2009; 324:1457-61; PMID:19460966; http://dx.doi.org/10.1126/science.1171362
32. Rhim AD, Oberstein PE, Thomas DH, Mirek ET, Palermo CF, Sastra SA, Dekleva EN, Saunders T, Becerra CP, Tattersall IW et al. Stromal elements act to restrain, rather than support, pancreatic ductal adenocarcinoma. Cancer Cell 2014; 25:735-47; PMID:24856585; http://dx.doi.org/10.1016/j.ccr.2014.04.021
33. Ozdemir BC, Pentcheva-Hoang T, Carstens JL, Zheng X, Wu CC, Simpson TR, Laklai H, Sugimoto H, Kahlert C, Novitskiy SV et al. Depletion of carcinoma-associated fibroblasts and fibrosis induces immunosuppression and accelerates pancreas cancer with reduced survival. Cancer Cell 2014; 25:719-34; PMID:24856586; http://dx.doi.org/10.1016/j.ccr.2014.04.005
34. Tomaino B, Cappello P, Capello M, Fredolini C, Sperduti I, Migliorini P, Salacone P, Novarino A, Giacobino A, Ciuffreda L et al. Circulating autoantibodies to phosphorylated α-enolase are a hallmark of pancreatic cancer. J Proteome Res 2011; 10:105-12; PMID:20455595; http://dx.doi.org/10.1021/pr100213b
35. Tran DQ. TGF-β: the sword, the wand, and the shield of FOXP3(+) regulatory T cells. J Mol Cell Biol 2012; 4:29-37; PMID:22158907; http://dx.doi.org/10.1093/jmcb/mjr033